Ballottin et al. Nanoscale Research Letters (2016) 11:313
DOI 10.1186/s11671-016-1538-y

Nanoscale Research Letters

NANO EXPRESS Open Access

Elucidating Protein Involvement in the Stabilization of the Biogenic Silver Nanoparticles

Daniela Ballottin[1,2], Stephanie Fulaz[1], Michele L. Souza[3,4], Paola Corio[3], Alexandre G. Rodrigues[5], Ana O. Souza[5], Priscyla M. Gaspari[6], Alexandre F. Gomes[7], Fábio Gozzo[7] and Ljubica Tasic[1,2*]

Abstract

Silver nanoparticles (AgNPs) have been broadly used as antibacterial and antiviral agents. Further, interests for green AgNP synthesis have increased in recent years and several results for AgNP biological synthesis have been reported using bacteria, fungi and plant extracts. The understanding of the role and nature of fungal proteins, their interaction with AgNPs and the subsequent stabilization of nanosilver is yet to be deeply investigated. Therefore, in an attempt to better understand biogenic AgNP stabilization with the extracellular fungal proteins and to describe these supramolecular interactions between proteins and silver nanoparticles, AgNPs, produced extracellularly by *Aspergillus tubingensis*—isolated as an endophytic fungus from *Rizophora mangle*—were characterized in order to study their physical characteristics, identify the involved proteins, and shed light into the interactions among protein-NPs by several techniques. AgNPs of around 35 nm in diameter as measured by TEM and a positive zeta potential of +8.48 mV were obtained. These AgNPs exhibited a surface plasmon resonance (SPR) band at 440 nm, indicating the nanoparticles formation, and another band at 280 nm, attributed to the electronic excitations in tryptophan, tyrosine, and/or phenylalanine residues in fungal proteins. Fungal proteins were covalently bounded to the AgNPs, mainly through S–Ag bonds due to cysteine residues (HS–) and with few N–Ag bonds from H_2N– groups, as verified by Raman spectroscopy. Observed supramolecular interactions also occur by electrostatic and other protein–protein interactions. Furthermore, proteins that remain free on AgNP surface may perform hydrogen bonds with other proteins or water increasing thus the capping layer around the AgNPs and consequently expanding the hydrodynamic diameter of the particles (~264 nm, measured by DLS). FTIR results enabled us to state that proteins adsorbed to the AgNPs did not suffer relevant secondary structure alteration upon their physical interaction with the AgNPs or when covalently bonded to them. Eight proteins in the AgNP dispersion were identified by mass spectrometry analyses. All these proteins are involved in metabolic pathways of the fungus and are important for carbon, phosphorous and nitrogen uptake, and for the fungal growth. Thereby, important proteins for fungi are also involved in the formation and stabilization of the biogenic AgNPs.

Keywords: Biogenic silver nanoparticles (AgNPs), Capping proteins, *Aspergillus tubingensis*

* Correspondence: ljubica@iqm.unicamp.br
[1]Laboratório de Química Biológica, Instituto de Química, Universidade Estadual de Campinas, Campinas, SP, Brazil
[2]NanoBioss, SisNano, Universidade Estadual de Campinas, Campinas, SP, Brazil
Full list of author information is available at the end of the article

Background

Nanotechnology has attracted the attention of researchers worldwide because of the unique properties of nanomaterials. Countless applications have been studied in different fields, such as medicine [1, 2], material science [3], microelectronics [4], energy storing [5], and biomedical devices [6].

Silver nanoparticles (AgNPs) have been largely employed in antibacterial and antiviral applications [7–16]. They present antibacterial and antimicrobial activity against Gram-negative and Gram-positive bacteria and some viruses as well [17–19]. Silver ions attack several targets in the bacteria making the development of resistance difficult [20]. The enormous surface area of nanoparticles improves its penetrability into the cell, enhancing their antimicrobial action [21].

AgNPs can be produced by chemical [22, 23], physical or biological routes [24, 25]. Biological synthesis uses clean routes, without producing toxic residues. AgNP biosynthesis can be performed using bacteria [7, 26], fungi [27–30], yeasts [31], plant extracts [32, 33], cyanobacteria [34], algae [35, 36], and actinomycetes [37]. This synthesis can be extra- or intra-cellular [38–41].

Fungi are easy microorganisms to manipulate as they grow in mycelial form; they are more resistant facing adverse conditions and provide a cost-effective large-scale production [42]. For these reasons, fungi appear to be interesting microorganisms for the green synthesis of silver nanoparticles. Fungus *Aspergillus tubingensis* is part of the black Aspergilli as well as *A. niger*, *A. carbonarius*, and *A. aculeatus* [24, 41–46] that grows on plant material. Many species of *Aspergillus* section *nigri* exhibit important biochemical differences in secretome [47–49]. *A. tubingensis*, used in this instance, was isolated as an endophytic fungus from *Rizophora mangle* [28]. Similar to other fungi, *A. tubingensis* is unable to import polymeric compounds into the cell and relies on enzymatic degradation to produce monomers or oligomers from different plant polymers among which polysaccharides are the major constituents [50, 51]. Due to structural differences in the plant polysaccharides, their effective degradation depends on an efficient system that regulates the production and secretion of different enzyme cocktails.

A. tubingensis is normally grown in a rich medium, such as potato dextrose agar (PDA), removed from it and washed with clean and distilled water originating the fungal filtrate (FF), rich in proteins and fungal metabolites. Then, Ag(I) aqueous solution is added into the FF where redox reactions occur and AgNPs are formed [51, 52]. Although various investigations have reported the mechanism of production of AgNPs obtained through this extracellular synthesis using different biological agents [33, 38–40], little is yet known about the role and nature of fungal proteins and also about their interactions with AgNPs and the subsequent stabilization of the as-produced nanosilver [51–55].

Interactions between nanosilver and proteins lead to AgNP stabilization and the formation of nanoparticle-biomolecular-capped structures [56–58] that could be monitored by different techniques. These biophysical and biochemical interactions occur through covalent bonds and electrostatic interactions [59, 60]. Silver nanoparticles can be complexed with the thiol HS– (Cys) or amine H_2N– groups [61–63] of the proteins and through electrostatic interactions [64] that have less impact on protein conformation and function. Sometimes, proteins covalently bound to AgNPs attract other proteins in order to form protein–protein-specific or nonspecific interactions that are an important part of the nanosilver-protein multilayer.

In an attempt to better understand biogenic AgNP stabilization with extracellular fungal proteins and to define these supramolecular interactions, we have chosen biogenic nanosilver with positive zeta potential. To the best of our knowledge, the present study is the first to report such data on covalently bound proteins to bionanosilver (AgNPs), synthesized by *A. tubingensis*. Biogenic AgNPs, of well-defined size and distinct morphology, are formed through the reduction of an aqueous solution of Ag(I) by a fungal filtrate.

Although the involvement of proteins in the reduction of the Ag(I) ions and the stabilization of a newly formed AgNPs has been described [23, 28, 64, 65], data about the way these proteins act are scarce. To fill the gap, the present study was devised in order to identify the proteins that promote the formation of AgNPs and those involved in the stabilization of the same nanomaterials.

Methods

All chemicals used in this study were purchased from Sigma-Aldrich (St. Louis, MO, USA) and used without further purification unless otherwise stated.

Fungal strain of *A. tubingensis* (AY876924) was provided by I. S. Melo (Embrapa/CNPMA, Brazil) and is part of the culture collection of the "Embrapa Recursos Genéticos e Biotecnologia (CENARGEN)" in the "Collection of Microorganisms for Biocontrol of Plant Pathogens and Weeds" (http://mwpin004.cenargen.embrapa.br/jrgnweb/jmcohtml/jmcoconsulta-externa.jsp?idcol=11) under the number CEN1065.

Silver Nanoparticle Synthesis

The endophytic fungi *A. tubingensis* was cultivated in potato dextrose agar medium (PDA) at 28 °C for 7 days. Afterwards, the fungal colonies were transferred to tubes containing 5 mL of saline solution (9 % NaCl). The obtained suspension was added to 150 mL of potato

dextrose broth (PDB) in a 1-L Erlenmeyer flask and incubated in an orbital shaker (Marconi MA420, Brazil) at 25 °C and 150 rpm for 72 h. After this period, the biomass was filtered using a polypropylene membrane and washed with sterile water. After incubation with sterile water at 25 °C and 150 rpm for 72 h, the biomass was removed and the fungal filtrate (FF) was obtained using a cellulose acetate membrane of 0.22 μm.

For AgNP synthesis, 1 mL of $AgNO_3$ solution (0.1 mol L^{-1}), previously filtered through a cellulose regenerated membrane (0.22 μm), was added to 99 mL of the FF to reach a final concentration of 1 mmol L^{-1}. The flask was kept at 25 °C and protected in dark for 96 h. The formation of AgNPs was monitored using a UV-Vis spectrophotometer (Agilent 8453). Control (FF without any silver ions) was used as blank. The average size (z-average) of AgNPs was measured by dynamic light scattering (DLS) (Nano ZS Zetasizer, Malvern Instruments Corp, UK) at 25 °C in polystyrene cuvettes with a path length of 10 mm. The zeta potential was measured in capillary cells with a path length of 10 mm, using the same instrument. The samples were diluted with 0.1 mmol L^{-1} NaCl before the analysis.

Characterization of the Proteins Capping the AgNPs

FTIR spectroscopy measurements were carried out from KBr tablets of two samples, AgNPs and FF, and were recorded in an ABB Bomem (MB series, USA) instrument with a resolution of 4.0 cm^{-1} and in an interval from 4000 to 400 cm^{-1}.

Raman spectroscopy measurements were implemented at the Instituto de Química, Universidade de São Paulo and recorded in a Renishaw InVia Reflex equipment coupled to a DM2500M Leica microscope using 632.8 and 785 nm lasers at 3 mW and 30 mW, respectively. Fifty-second accumulation in a total of three scans to each sample between 100 and 1800 cm^{-1} range were obtained, at 4 cm^{-1} resolution. All samples were analyzed in suspension and solid KCl was added in order to promote aggregation; however, no visual change was noticed.

LC-MS/MS analysis were performed at Laboratório Dalton, Instituto de Química, Universidade Estadual de Campinas using a nanoACQUITY chromatograph with a UPLC (Waters) coupled to a Synapt HDMS spectrometer (Waters) with QTOF geometry equipped with a nanoESI source operating in the acquisition-dependent data mode (ADD).

After being quantified by the Bradford method [66], proteins from the FF and linked to the AgNPs were analyzed by LC-MS/MS according to a method based on denaturation followed by digestion using the trypsin enzyme (Sequencing Grade Modified Trypsin, Promega), desalting and concentration. The resulting solutions were centrifuged (10 min at 17,000×*g*) and the supernatant was transferred into appropriate vials. Then, the samples were injected into the UPLC system, first passing through the precolumn (Waters Symmetry C18, 20 mm × 180 μm, particles 5 μm), being desalted during 3 min with a flow of 5.0 μL min^{-1} with 97:3 water/acetonitrile with 0.1 % formic acid (v/v) and, afterwards, they were transferred to the analytical column (Waters C18 BEH130, 100 mm ID × 100 μm, particles of 1.7 μm). Finally, the samples were eluted with a flow rate of 1.0 μL min^{-1} by varying the gradient of mobile phases with a gradient of buffer A (water/formic acid 0.1 %, v/v) and B (acetonitrile/formic acid 0.1 %, v/v) at the rates of 97:3, 70:30, 20:80, 20:80, 97:3, and 97:3 at 0, 40, 50, 55, 56, and 60 min, respectively. The identification of the peptides was done using the online version of the Waters software with a mass spectrometer (Synapt HDMS-Waters) configured to operate in dependent acquisition data (ADD) mode containing a function MS full-scan (*m/z* 200–2000), a three function fragment ion spectrum (MS/MS, m/z 50 to 50 units over the m/z of the precursor) and a function of external standard calibration (lock-mass, m/z 200–2000). All spectra were acquired at a rate of 1 Hz. The other parameters were capillary voltage of 3.0 kV, cone voltage of 30 V, source temperature of 100 °C Gas Flow nanoESI 0.5 L h^{-1}, collision energies of 6:04 eV and a 1700-V detector. The acquisition of raw data was performed with ProteinLynx Global Server v.2.2 software (Waters). Data treatments for the deconvolutions of raw spectra were performed with Transform software (Micromass, UK). MASCOT v.2.2 system (Matrix Science Ltd. http://www.matrixscience.com). Data banks were searched in order to identify the fungal proteins.

Results and Discussion

Biogenic AgNP formation through a fungal-based extracellular synthesis is a known, efficient, green, and relatively fast way for AgNP production [28, 58, 61, 62, 65, 67, 68] as this process takes a few days to complete (Fig. 1a). Herein, the biogenic synthesis was monitored by UV-Vis spectroscopy (Fig. 1b). The formation of AgNPs was completed within 72 h after the FF was challenged with $AgNO_3$, in good agreement with what was previously reported [28]. The UV-Vis spectrum displays two main bands, an SPR band at 440 nm, characteristic of the AgNP presence, and an additional band at 280 nm, which could be attributed to the aromatic amino acids of the capping proteins [69]. It is well-known that the absorption band in this region arises due to the electronic excitations in tryptophan, tyrosine and/or phenylalanine residues in fungal proteins [69–71]. These results confirm the AgNPs formation and the presence of fungal proteins.

Silver nanoparticles were characterized, and their average diameter and zeta potential were evaluated. In DLS analysis, these AgNPs showed a hydrodynamic diameter of 264.9 ± 3.2 nm and relatively low polydispersity (0.32)

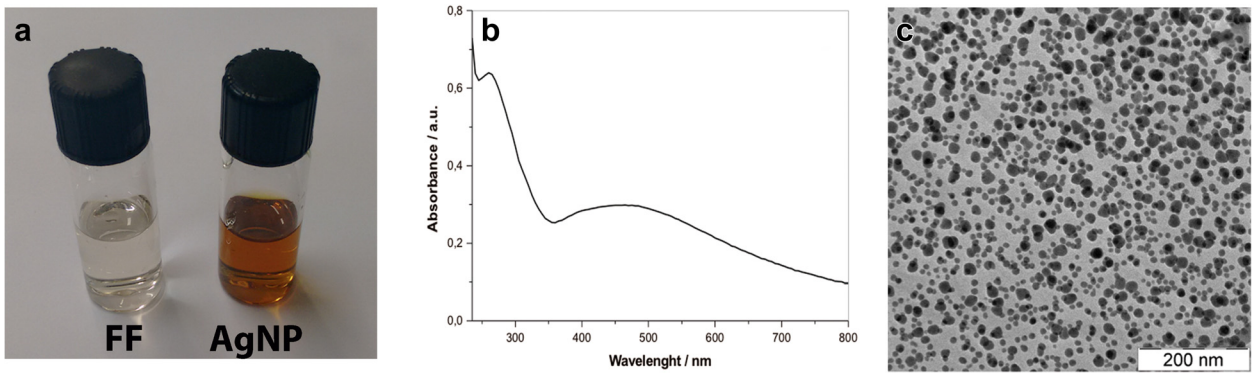

Fig. 1 **a** Image of the fungal filtrate and the AgNP suspension. **b** UV-Vis spectra obtained for AgNP suspension using FF as blank. **c** Electronic Transmission micrograph showing the AgNPs

(data not shown herein, already presented in [28]). Their zeta potential was positive with a value of + 8.48 ± 0.45 mV which could be indicative of low-charged surfaces and, consequently, unstable AgNPs [72], contrary to what was observed during a 6-month period. The high AgNPs stability might be attributed to the fungal protein-capping around the particles what confers them steric stability. The average diameter measured by TEM was 35 ± 10 nm (Fig. 1b and other data shown previously [28]). This value is smaller when compared to that measured by DLS, because in the latter technique the hydrodynamic diameter (particles and stabilization protein-capping) is taken into account [28], on the other hand, TEM allows the measurement of the AgNP diameter without the surrounding capping layers. Once again, strong evidence for fungal proteins linked to the silver nanoparticles was obtained.

Protein adsorption on the surface of biogenic AgNPs was also confirmed by FTIR spectroscopy (Fig. 2). For example, the peptide bond exhibits characteristic bands denominated amide A, B, I-VII. The Fermi resonance that occurs among the first overtone of amide II and the N–H stretching vibration create the bands amide A (about 3500 cm^{-1}) and amide B (about 3100 cm^{-1}) [72–76]. The band in 1600–1700 cm^{-1} named amide I is related with the C = O stretching vibration from the backbone conformation [72]. The amide II band arises from the N–H bending vibration and from the C–N stretching vibration [73] and is conformational sensitive. The complex bands

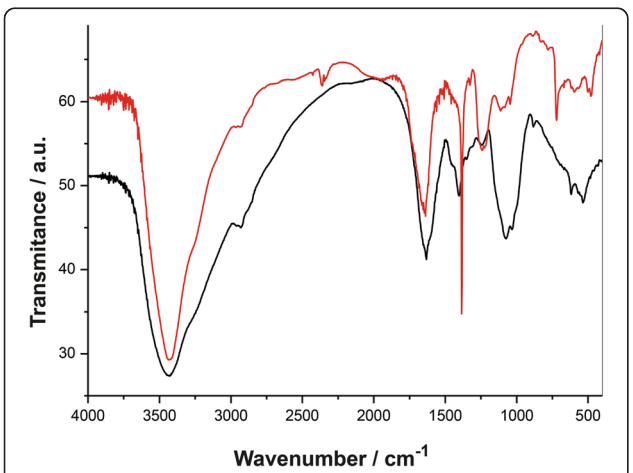

Fig. 2 FTIR spectra of the fungal filtrate (*black*) and AgNPs (*red*) carried out in KBr tablets

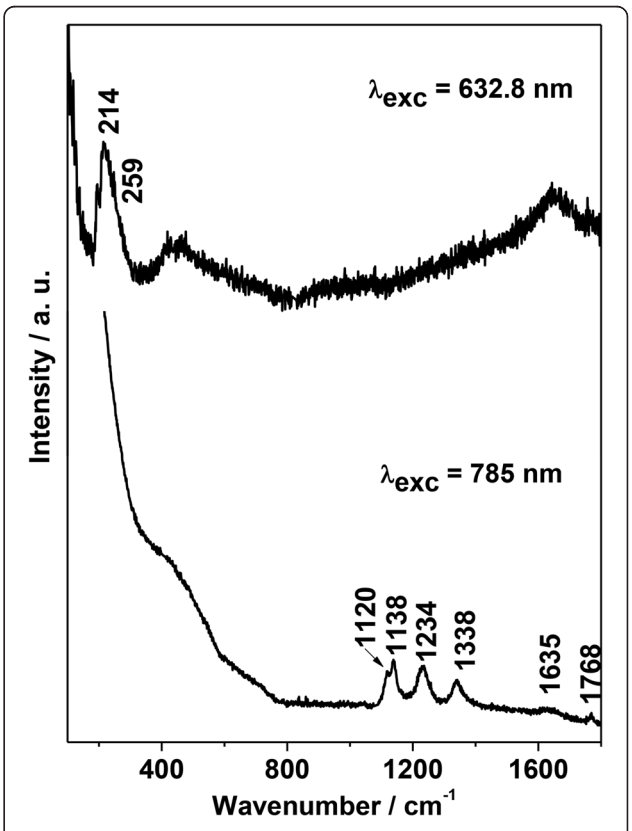

Fig. 3 Raman spectra of AgNPs recorded with laser excitations of 632.8 nm and 785 nm. The main wavenumbers discussed further in text are pointed

Amide III and IV originates from a mixture of several coordinate displacements [77]. The symmetric and asymmetric vibrations of the C–H groups result in bands at 2920–2950 cm^{-1}, respectively [78], while bands at 1620 to 1650 cm^{-1} are attributed to –C(O)– of peptide bonds and/or $–NH_2$ groups and those at 1380–1030 cm^{-1} to C-N bonds [74, 75].

According to the FTIR results the proteins on AgNP surface did not undergo relevant secondary structure alteration along with their interaction with AgNPs, nor when covalently bonded to them as reported in other published data [50, 51]. The interaction between the proteins and AgNPs might be covalent bound to the amino groups, cysteine residues, and/or electrostatic interactions via carboxyl groups.

The Raman spectra (Fig. 3) indicate the presence of protein-capping at the surface of the investigated AgNPs [77, 79, 80], confirming the DLS results for the hydrodynamic diameter. Moreover, Raman spectroscopy enable observe if the protein binding to the surface occurs via free amino groups or through cysteine residues. The spectrum excited at 632.8 nm presents little vibrational information about the molecules at the AgNP surface. The broad band at around 214 cm^{-1} can be assigned to an overlap between the Ag–Cl vibration (given the presence of Cl–) and an Ag–S vibration suggesting an interaction between superficial Ag and the cysteine (HS–) group of the capping proteins. When the samples were excited at 785 nm, strong bands assigned to the adsorbed proteins are observed at 1338 and 1768 cm^{-1}, assigned to the amide III and amide I modes, respectively, as already discussed in the FTIR results above. Bands at 1120 and 1138 cm^{-1} are assigned to NCH stretching and CCH bending modes, respectively, and 1234 cm^{-1} to vibrations in antiparallel β-sheet in the protein structure [81]. A broad and weak band related to the amide II mode is present at approximately 1635 cm^{-1}, which was expected to be at lower frequencies (below 1600 cm^{-1}). The observed blue shift is associated to a response of the protein bonding to AgNPs, increasing the vibrational frequencies of the free amine II mode. On the other hand, it was expected to detect HCS bending between 800 and 900 cm^{-1}. However, such peak was not present in any of the obtained spectra reinforcing that the binding of protein to the AgNP surface occurred mainly

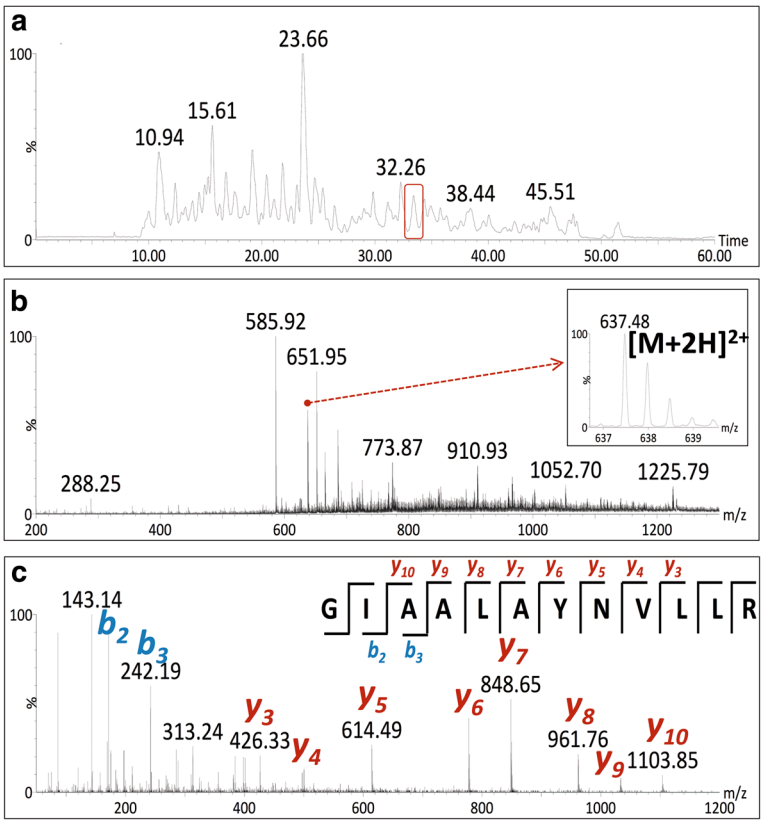

Fig. 4 Illustration of the data obtained in performed MS/MS analysis. **a** The chromatogram is showing the eluation times for the AgNPs trypsin-hydrolyzed sample where sample's peptides are given from 0 to 50 min; the peptide (*red box*) at 32.26 min was selected for posterior identification in MS. **b** Mass spectrum that corresponds to the peptide from 32.26 min (*red box* in **a**). **c** MS/MS data and procedure followed for the identification of the peptide sequence for the peptide from 32.26 min (*red box* in **a**)

through the –SH groups. In such case, the amino group remains free and may perform hydrogen bonds with other proteins or water, contributing hence to the large hydrodynamic radius and the low charge surface of these NP. Therefore, proteins detected in AgNPs are covalently bound to the silver through S–Ag bonds, principally, and with some adhered proteins via electrostatic or other protein–protein interactions.

The protein identification in the dispersion of AgNPs was performed starting from the protein tryptic lysis followed by LC-MS/MS analysis [82–88]. An illustration of the LC-MS/MS results obtained for proteins capping AgNPs is shown in Fig. 4 and all identified proteins are shown in Additional file 1: Table S1. The most intense signals in the chromatograms of peptides were selected for further fragmentation and, after obtaining their MS spectra, three to five most intense m/z ions were fragmented in MS/MS spectra allowing us to associate an amino acid sequence for a fragmentation pattern, as exemplified for one of the identified peptides (Fig. 4).

Mass spectrometry analyses enabled the identification of eight (8) proteins in the AgNPs dispersion and these are presented in Additional file 1: Table S1. All of them, secreted by *A. tubingensis*, display low isoelectric points, ranging from 4.0 to 5.1, characteristic for acidic proteins. Their molecular masses varied from 39 to 65.5 kDa.

A. tubingensis was grown in broth whose pH was 6.5 to 6.8 and, therefore, the fungus extracellular proteins should exhibit negative charge due to the deprotonation, which could increase the zeta potential of the synthetized AgNPs. Nevertheless, the positive zeta potential of approximately 8 mV, which should be indicative of low-charged surfaces, is probably a consequence of these protein-capping deprotonation. Some published data on chemical AgNPs and protein interactions also report similar observations [50].

Among identified proteins, we have found glycoamilase (1,4-α-D-glucanglucohydrolase, EC 3.2.1.3), acid phosphatase (EC 3.1.3.2), serine carboxipeptidase (EC 3.4.21.26), and glucanosyltransferase (EC 2.4) that are illustrated in Fig. 5. All these proteins are involved in metabolic pathways of the fungi and belong to hydrolases [56, 89–93], important for carbon, phosphorous, and nitrogen uptake, respectively, and for the fungal growth. Furthermore, all identified hypothetic proteins also constitute the secretome of *A. tubingensis*. Although of unknown function, these proteins, which contain the signaling sequences at the N-terminal, are always secreted, and their probable functions are associated with metabolic supplies.

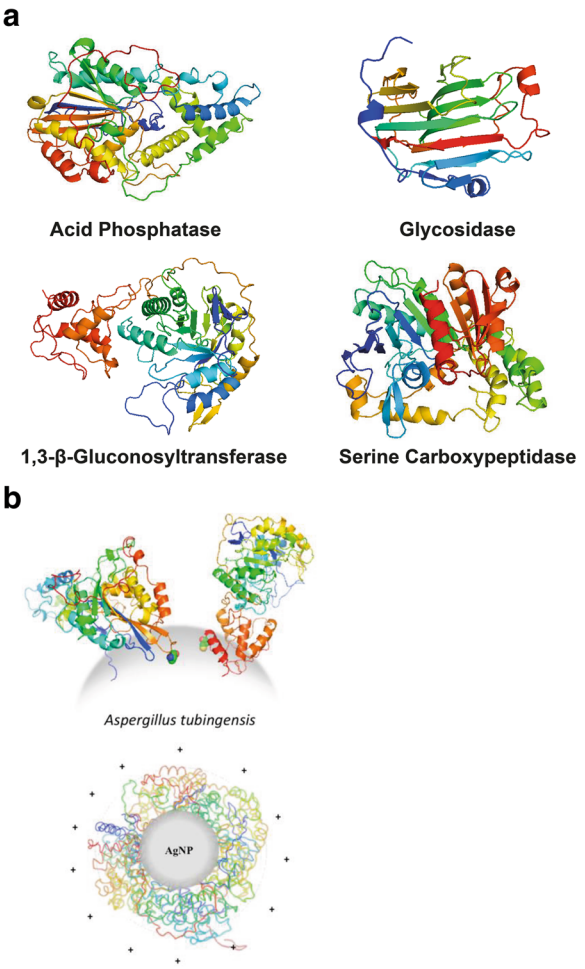

Fig. 5 **a** Illustration of the 3D structures (in *ribbon*) of the most important biogenic AgNP proteins identified using MS/MS in biogenic AgNP characterization. **b** Representation of the proteins around the AgNPs

Conclusions

Silver nanoparticles were biosynthesized using the secreted proteins from the fungus *A. tubingensis*. This fungal filtrate in contact with $AgNO_3$ produced within 72 h AgNPs with 264.9 ± 3.2 nm in the hydrodynamic diameter, 35 ± 10 nm in the nanoparticle diameter and with a zeta potential of + 8.48 ± 0.45 mV. The nanoparticle formation was followed by UV-Vis spectroscopy, and the increase in the intensity of the SPR band was observed during AgNPs synthesis. The presence of fungal proteins in the AgNPs dispersion was verified by all spectrometric and spectroscopic analyses used. The FTIR along with the Raman data enabled us to identify the amino I, II, and III bands of proteins adhered to AgNP surface. Proteins formed covalent bonds with atoms at the surface of AgNPs surface due to their cysteine residues (Ag–S bonds) most likely. Secondary and tertiary structure features of proteins were preserved even when they were chemically bound to Ag atoms at the surface of the NPs. Eight proteins from *A. tubingensis* secretome were identified by MS/MS. All data collected and analyzed

strongly indicate that not all fungal proteins bind to the formed AgNPs. However, some proteins enable the synthesis of AgNPs and provide stability to the formed nanosilver, not only through covalent bonds, but also due to attraction of other proteins through hydrogen bonds, electrostatic, or other supramolecular interactions, forming a multilayer, as evidenced by zeta potential measurements and size determinations of the AgNPs.

Availability of Data and Materials

Mass spectrometry data treatments for the deconvolutions of raw spectra were performed with Transform software (Micromass, UK). MASCOT v.2.2 system (Matrix Science Ltd. http://www.matrixscience.com) and the data bank (UniProt http://www.uniprot.org/) searches were done in order to identify fungal proteins.

Additional File

Additional file 1: Table S1. *Aspergillus tubingensis* identified protein in the silver nanoparticles (AgNP) capping using LC-MS/MS. (DOC 58 kb)

Abbreviations

ADD, acquisition-dependent data; Ag, silver; AgNP, silver nanoparticles; DLS, dynamic light scattering; FF, fungal filtrate; FTIR, Fourier transform infrared spectroscopy; QTOF, quadrupole time-of-flight; TEM, transmission electron microscopy; UPLC, ultra performance liquid chromatography

Competing Interests

The authors declare that they have no competing interests.

Authors' Contributions

DB contributed by developing the study, analysis and interpretation of the results. PG and AO contributed to the analysis and interpretation of the results. SF carried out the manuscript preparation and data organization. PC and MS realized the Raman spectroscopy experiments and data interpretation. FG and AG performed the mass spectrometry analysis. DB and LT worked on the protein identification and characterization. LT has contributed in designing the study, supervising the experiments, understanding the results, and reviewing the manuscript. All authors read and approved the final manuscript.

Acknowledgements

We thank the *Fundação de Amparo à Pesquisa do Estado de São Paulo* (FAPESP, São Paulo, Brazil, Grants's Numbers: 2010/14584-5, 2011/00222-8 and 2012/13119-3) and *Conselho Nacional de Desenvolvimento Científico e Tecnológico* (CNPq, Brasília, Brazil) for financial supports and fellowships. And last, but not the least, we express our gratitude to Dr. Dahoumane who has carefully read and corrected our manuscript, thus making it more readable, and also for all given suggestions and comments.

Author details

[1]Laboratório de Química Biológica, Instituto de Química, Universidade Estadual de Campinas, Campinas, SP, Brazil. [2]NanoBioss, SisNano, Universidade Estadual de Campinas, Campinas, SP, Brazil. [3]Departamento de Química Fundamental, Instituto de Química, Universidade de São Paulo, São Paulo, SP, Brazil. [4]Instituto de Ciências Exatas, Universidade Federal Fluminense, Volta Redonda, RJ, Brazil. [5]Laboratório de Bioquímica e Biofísica, Instituto Butantan, São Paulo, SP, Brazil. [6]Laboratório de Nanobiotecnologia, Faculdade de Ciências Farmacêuticas, Universidade de São Paulo, Riberão Preto, SP, Brazil. [7]Laboratório Dalton, Instituto de Química, Universidade Estadual de Campinas, Campinas, SP, Brazil.

Received: 15 March 2016 Accepted: 24 June 2016
Published online: 29 June 2016

References

1. Arun G, Eyini M, Gunasekaran P (2014) Green synthesis of silver nanoparticles using the mushroom fungus *Schizophyllum commune* and its biomedical applications. Biotechnol Bioprocess Eng 19:1083–1090
2. Sun T, Zhang YS, Pang B, Hyun DC, Yang M, Xia Y (2014) Engineered nanoparticles for drug delivery in cancer therapy. Angew Chem Int Ed 53: 12320–12364
3. Lu AH, Salabas EL, Schüth F (2007) Magnetic nanoparticles: synthesis, protection, functionalization and application. Angew Chem Int Ed 46:1222–4
4. Grisolia J, Viallet B, Amiens C, Baster S, Cordan AS, Leroy Y, Soldano C, Brugger J, Ressier L (2009) 99% random telegraph signal-like noise in gold nanoparticle μ-stripes. Nanotechnology 20:355303–9
5. Bullis K (2014) Nanoparticle networks promise cheaper batteries for storing renewable energy. MIT Technol Rev. http://www.technologyreview.com/news/526811/nanoparticle-networks-promise-cheaper-batteries-for-storing-renewable-energy/. Accessed 30 Sep 2015
6. Bajaj A, Miranda OR, Kim IB, Phillips RL, Jerry DJ, Bunz UHF, Rotello VM (2009) Detection and differentiation of normal, cancerous, and metastatic cells using nanoparticle-polymer sensor arrays. Proc Natl Acad Sci U S A 106:10912–6
7. Baker S, Kumar KM, Santosh P, Rakshith D, Satish S (2015) Extracellular synthesis of silver nanoparticles by novel *Pseudomonas veronii* AS41G inhabiting *Annona squamosa L.* and their bactericidal activity. Spectrochim Acta A Mol Biomol Spectrosc 136:1434–1440
8. Kuppusamy P, Ichwan SJA, Parine NR, Yusoff MM, Maniam GP, Govidan N (2015) Intracellular biosynthesis of Au and Ag nanoparticles using ethanolic extract of *Brassica oleracea L.* and studies on their physicochemical and biological properties. J Environ Sci 29:151–7
9. Logeswari P, Silambarasan S, Abraham J (2015) Synthesis of silver nanoparticles using plants extract and analysis of their antimicrobial property. J Saudi Chem Soc 19:311–7
10. Sinha SN, Paul D (2015) Phytosynthesis of silver nanoparticles using *andrographis paniculata* leaf extract and evaluation of their antibacterial activities. Spectrosc Lett 48:600–604
11. Velusamy P, Das J, Pachaiappan R, Vaseeharan B, Pandian K (2015) Greener approach for synthesis of antibacterial silver nanoparticles using aqueous solution of neem gum (*Azadirachta indica L.*). Ind Crops Prod 66:103–9
12. Tolaymat T, El Badawy AM, Genaidy A, Scheckel KG, Luxton TP, Suidan M (2010) An evidence-based environmental perspective of manufactured silver nanoparticle in synthesis and applications: a systematic review and critical appraisal of peer-reviewed papers. Sci Tot Environ 408:999–1006
13. Li WR, Xie XB, Shi QS, Zeng HY, Ou-Yang YS, Chen YB (2010) Antibacterial activity and mechanism of silver nanoparticles on *Escherichia coli*. Appl Microbiol Biotechnol 85:1115–1122
14. Gajbhiye M, Kesharwani J, Ingle A, Gade A, Rai M (2009) Fungus-mediated synthesis of silver nanoparticles and their activity against pathogenic fungi in combination with fluconazole. Nanomedicine 5:382–6
15. Lara HH, Garza-Trevino EN, Ixtepan-Turrent L, Singh DK (2011) Silver nanoparticles are broad-spectrum bactericidal and virucidal compounds. J Nanobiotech 9:8
16. Morones JR, Elechiguerra JL, Camacho A, Holt K, Kouri JB, Ramirez JT, Yacaman MJ (2005) The bactericidal effect of silver nanoparticles. Nanotechnology 16:2346–2353
17. Galdiero S, Falanga A, Cantisani M, Ingle A, Galdiero M, Rai M (2014) Silver nanoparticles a novel antibacterial and antiviral agents. In: Torchilin V (ed) Handbook of nanobiomedical research: fundamentals, applications and recent developments. World Scientific Publishing Company, Singapure, pp 565–594
18. Le Ouay B, Stellacci F (2015) Antibacterial activity of silver nanoparticles: a surface science insight. Nano Today 10:339–354
19. Lara HH, Ayala-Nuñez NV, Ixtepan-Turrent L, Rodriguez-Padilla C (2010) Mode of antiviral action of silver nanoparticles against HIV-1. J Nanobiotechnol 8:1
20. Pal S, Tak YK, Song JM (2007) Does the antibacterial activity of silver nanoparticles depend on the shape of the nanoparticle? A study of the Gram-negative bacterium *Escherichia coli*. Appl Environ Microbiol 73:1712–1720
21. Ravindran A, Chandran P, Khan SS (2013) Biofunctionalized silver nanoparticles: Advances and prospects. Colloids Surf B Biointerfaces 105:342–352

22. Ismail IM, Ewais HA (2015) Mechanistic and kinetic study of the formation of silver nanoparticles by reduction of silver(I) in the presence of surfactants and macromolecules. Transit Metal Chem 40:371–8
23. Lok CN, Ho CM, Chen R, He QY, Yu WY, Sun HZ, Tam PKH, Chiu JF, Che CM (2006) Proteomic analysis of the mode of antibacterial action of silver nanoparticles. J Proteome Res 5:916–924
24. Prabhu S, Poulose EK (2012) Silver nanoparticles: mechanism of antimicrobial action, synthesis, medical applications, and toxicity effects. Int Nano Lett 2:32
25. Iravani S, Korbekandi H, Mirmohammadi SV, Zolfaghari B (2014) Synthesis of silver nanoparticles: chemical, physical and biological methods. Res Pharm Sci 9:385–406
26. Deepak V, Kalishwaralal K, Pandian SRK, Gurunathan S (2011) An Insight into the bacterial biogenesis of silver nanoparticles, industrial production and scale-up. In: Rai M, Duran N (eds) Metal nanoparticles in microbiology. Sringer-Verlag, Berlin, pp 17–35
27. Gupta IR, Anderson AJ, Rai M (2015) Toxicity of fungal-generated silver nanoparticles to soil-inhabiting *Pseudomonas putida* KT2440, a rhizospheric bacterium responsible for plant protection and bioremediation. J Hazard Mater 286:48–54
28. Rodrigues AG, Ping LY, Marcato PD, Alves OL, Silva MCP, Ruiz RC, Melo IS, Tasic L, De Souza AO (2013) Biogenic antimicrobial silver nanoparticles produced by fungi. Appl Microbiol Biotechnol 97:775–782
29. Krijsheld P, Altelaar AFM, Post H, Ringrose JH, Muller WH, Heck AJR, Wosten HAB (2012) Spatially resolving the secretome within the mycelium of the cell factory *Aspergillus niger*. J Proteome Res 11:2807–2818
30. Raliya R, Tarafdar JC (2012) Novel Approach for silver nanoparticle synthesis using *Aspergillus terreus* CZR-1: mechanism perspective. J Bionanosci 6:1–5
31. Apte M, Sambre D, Gaikawad S, Joshi S, Bankar A, Kumar AR, Zinjarde S (2013) Psychrotrophic yeast *Yarrowia lipolytica* NCYC 789 mediates the synthesis of antimicrobial silver nanoparticles via cell-associated melanin. AMB Express 3:32
32. Hyllested JA, Palanco ME, Hagen N, Mogensen KB, Kneipp K (2015) Green preparation and spectroscopic characterization of plasmonic silver nanoparticles using fruits as reducing agentes. Beilstein J Nanotechnol 6:293–9
33. Sadeghi B, Gholamhoseinpoor F (2015) A study on the stability and green synthesis of silver nanoparticles using *Ziziphora tenuior* (Zt) extract at room temperature. Spectrochim Acta A Mol Biomol Spectrosc 134:310–5
34. Brayner R, Barberousse H, Hemadi M, Djedjat C, Yéprémian C, Coradin T, Livage J, Fiévet F, Couté A (2007) Cyanobacteria as bioreactors for the synthesis of Au, Ag, Pd, and Pt nanoparticles via an enzyme-mediated route. J Nanosci Nanotech 1:2696–2708
35. Dahoumane SA, Wijesekera K, Filipe CDM, Brennan JD (2014) Stoichiometrically controlled production of bimetallic gold-silver alloy colloids using micro-alga cultures. J Colloid Interface Sci 416:67–72
36. Xie J, Lee JY, Wang DIC, Ting YP (2007) Silver nanoplates: from biological to biomimetic synthesis. ACS Nano 1:429–439
37. Abdeen S, Geo S, Sukanya, Praseetha PK, Dhanya RP (2014) Biosynthesis of silver nanoparticles from Actinomycetes for therapeutic applications. Int J Nano Dimens 5:155–162
38. Rai MK, Deshmukh SD, Ingle AP, Gade AK (2012) Silver nanoparticles: the powerful nanoweapon against multidrug-resistant bacteria. J Appl Microbiol 112:841
39. Otari SV, Patil RM, Ghosh SJ, Thorat ND, Pawar SH (2015) Intracellular synthesis of silver nanoparticle by actinobacteria and its antimicrobial activity. Spectrochim Acta A Mol Biomol Spectrosc 136:1175–1180
40. Gupta VK, Mach RL, Sreenivasaprasad S (2015) Fungal Biomolecules: sources, applications and recent developments. 1st ed. Wiley-Blackwell, India, pp 117–136
41. Bhainsa KC, D'Souza SF (2006) Extracellular biosynthesis of silver nanoparticles using the fungus *Aspergillus fumigatus*. Colloids Surf B Biointerfaces 47:160
42. Adkins Y, Lennard B (2004) Proteins and peptides. In: Neeser JR, German JB (eds) Bioprocesses and biotechnology for functional foods and nutraceuticals. Marcel Dekker INC, New York, pp 149–174
43. Mohanpuria P, Rana NK, Yadav SK (2008) Biosynthesis of nanoparticles: technological concepts and future applications. J Nanopart Res 10:507–517
44. Mukherjee P, Ahmad A, Mandal D, Senapati S, Sainkar S, Khan MI, Parischa R, Ajaykumar PV, Alam M, Kumar R, Sastry M (2001) Fungus-mediated synthesis of silver nanoparticles and their immobilization in the mycelial matrix: a novel biological approach to nanoparticle synthesis. Nano Lett 1:515–519
45. Iravani S (2011) Green synthesis of metal nanoparticles using plants. Green Chem 13:2638–2650
46. http://genome.jgi.doe.gov/Asptu1/Asptu1.home.html. Accessed 05 May 2016
47. Agnihotri S, Mukherji S, Mukherji S (2013) Immobilized silver nanoparticles enhance contact killing and show highest efficacy: elucidation of the mechanism of bactericidal action of silver. Nanoscale 5:7328–7340
48. Kim JS, Kuk E, Yu KN, Kim JH, Park SJ, Lee HJ, Kim SH, Park YK, Park YH, Hwang CY, Kim YK, Lee YS, Jeong DH, Cho MH (2007) Antimicrobial effects of silver nanoparticles. Nanomedicine 3:95–101
49. Klaus T, Joerger R, Olsson E, Granvqist CG (1999) Silver-based crystalline nanoparticles, microbially fabricated. Proc Natl Acad Sci U S A 96:13611–4
50. Käkien A, Ding F, Chen P, Mortimer M, Kahru A, Ke PC (2013) Interaction of firefly luciferase and silver nanoparticles and its impact on enzyme activity. Nanotechnology 24:345101
51. Banerjee V, Das KP (2013) Interaction of silver nanoparticles with proteins: a characteristic protein concentration dependent profile of SPR signal. Colloids Surf B Biointerfaces 111:71–9
52. Bondarenko O, Ivask A, Kakinen A, Kurvet I, Kahru A (2013) Particle-cell contact enhances antibacterial activity of silver nanoparticles. PLoS One 8:64060
53. Quaresma P, Soares L, Contar L, Miranda A, Osorio I, Carvalho P, Franco R, Pereira E (2009) Green photocatalytic synthesis of stable Au and Ag nanoparticles. Green Chem 11:1889–1893
54. Korbekandi H, Iravani S, Abbasi S (2012) Optimization of biological synthesis of silver nanoparticles using *Lactobacillus casei* subsp. casei. J Chem Technol Biotechnol 87:932–7
55. Narayanan KB, Sakthivel N (2010) Biological synthesis of metal nanoparticles by microbes. Adv Colloid Interfac 156:1–13
56. Christakopoulos P, Kekos D, Macris BJ, Claeyssens M, Bhat MK (1995) Purification and mode of action of a low molecular mass endo-1,4-β-D-glucanase from *Fusarium oxysporum*. J Biotechnol 39:85–93
57. Christakopoulos P, Nerinckx W, Kekos D, Macris B, Claeyssens M (1996) Purification and characterization of two low molecular mass alkaline xylanases from *Fusarium oxysporum*. J Biotechnol 51:181–9
58. Durán N, Marcato PD, De Conti R, Alves OL, Costa FTM, Brocchi M (2010) Potential use of silver nanoparticles on pathogenic bacteria, their toxicity and possible mechanisms of action. J Braz Chem Soc 21:949–959
59. Wen YM, Geitner NK, Chen R, Ding F, Chen PY, Andorfer RE, Govindan PN, Ke PC (2013) Binding of cytoskeletal proteins with silver nanoparticles. RSC Adv 3:22002–7
60. Chung YC, Chen IH, Chen CJ (2008) The surface modification of silver nanoparticles by phosphoryl disulfides for improved biocompatibility and intracellular uptake. Biomaterials 29:1807
61. Sharma VK, Yngard RA, Lin Y (2009) Silver nanoparticles: green synthesis and their antimicrobial activities. Adv Colloid Interface 145:83
62. Chaloupka K, Malam Y, Seifalian AM (2010) Nanosilver as a new generation of nanoproduct in biomedical applications. Trends Biotechnol 28:580
63. Aymonier C, Schlotterbeck U, Antonietti L, Zacharias P, Thomann R, Tiller JC, Mecking S (2002) Hybrids of silver nanoparticles with amphiphilic hyperbranched macromolecules exhibiting antimicrobial properties. Chem Commun (Camb) 8: 3018-9
64. Yamanaka M, Hara K, Kudo J (2005) Bactericidal actions of a silver ion solution on *Escherichia coli*, studied by energy-filtering transmission electron microscopy and proteomic analysis. Appl Environ Microbiol 71:7589–7593
65. Rai M, Yadav A, Gade A (2009) Silver nanoparticles as a new generation of antimicrobials. Biotechnol Adv 27:76–83
66. Bradford MM (1976) A rapid and sensitive method for the quantitation of microgram quantities of protein utilizing the principle of protein-dye binding. Anal Biochem 72:248–254
67. Durán N, Marcato PD, Durán M, Yadav A, Gade A, Rai M (2011) Mechanistic aspects in the biogenic synthesis of extracellular metal nanoparticles by peptides, bacteria, fungi, and plants. Appl Microbiol Biotechnol 90:1609–1624
68. Gaikwad SC, Birla SS, Ingle AP, Gade AK, Marcato PD, Rai M, Duran N (2013) Screening of different *Fusarium* species to select potential species for the synthesis of silver nanoparticles. J Braz Chem Soc 24:1974–1982
69. Toledo MAS, Santos CA, Mendes JS, Pelloso AC, Beloti LL, Crucello A, Favaro MTP, Santiago AS, Schneider DRS, Saraiva AM, Stach-Machado DR, Souza AA, Trivella DBB, Aparício R, Tasic L, Azzoni AR, Souza AP (1834) Small-angle X-ray scattering and *in silico* modelling approaches for the accurate functional annotation of an LysR-type transcriptional regulator. BBA Prot Proteom 2013:697–707

70. Oliveira C, Santos-Filho N, Menaldo D, Boldrini-França J, Giglio J, Calderon J, Stábeli R, Rodrigues F, Tasic L, Silva S, Soares A (2011) Structural and functional characterization of a γ-type phospholipase A2 inhibitor from *Bothrops jararacuçu* snake plasma. Curr Top Med Chem 11:2509–2519
71. Fattori J, Prando A, Assis LHP, Aparício R, Tasic L (2011) Structural insights on two hypothetical secretion chaperones from *Xanthomonas* axonopodis pv. citri. Protein J 6:126–135
72. Delgado AV, González-Caballero F, Hunter RJ, Koopal LK, Lyklema J (2005) Measurement and interpretation of electrokinetic phenomena. Pure Appl Chem 77:1753–1805
73. Treguer M, Rocco F, Lelong G, Nestour AL, Cardinal T, Maali A, Lounis B (2005) Fluorescent silver oligomeric clusters and colloidal particles. Solid State Sci 7:812–8
74. Germar FV, Galan A, Llorca O, Carrascosa JL, Valpuesta JM, Mantele W, Muga A (1999) Conformational changes generated in GroEL during ATP hydrolysis as seen by time-resolved infrared spectroscopy. J Biol Chem 274:5508–5513
75. Corbin J, Methot N, Wang HH, Baenziger JE, Blanton MP (1998) Secondary structure analysis of individual transmembrane segments of the nicotinic acetylcholine receptor by circular dichroism and fourier transform infrared spectroscopy. J Biol Chem 273:771
76. Haris PI, Chapman D (1995) The conformational analysis of peptides using fourier transform IR spectroscopy. Biopolymers 37:251–263
77. Pelton JP, McLean LR (2000) Spectroscopic methods for analysis of protein secondary structure. Anal Biochem 277:167–176
78. NiFu F, DeOlieveira DB, Trumble WR, Sarkar HK, Singh BR (1994) Secondary structure estimation of proteins using the Amide III region of fourier transform infrared spectroscopy: application to analyze calcium-binding-induced structural changes in calsequestrin. Appl Spectrosc 48:1432–1441
79. Tuma R (2005) Raman spectroscopy of proteins: from peptides to large assemblies. J Raman Spectrosc 36:307–319
80. George J, Thomas J (1999) Raman spectroscopy of protein and nucleic acid assemblies. Annu Rev Biophys Biomol Struct 28:1–27
81. Thomas GS (1977) Laser Raman scattering as a probe of protein structure. Ann Rev Biochem 46:553–557
82. Trauger SA, Webb W, Suizdak G (2002) Peptide and protein analysis with mass spectrometry. Spectroscopy 16:15–28
83. Tonack S, Neoptolemos JP, Costello E (2010) Analysis of serum proteins by LC-MS/MS. Methods Mol Biol 658:281–291
84. Kubota K, Kosaka T, Ichikawa K (2009) Shotgun protein analysis by liquid chromatography-tandem mass spectrometry. Methods Mol Biol 519:483–494
85. Wu CC, MacCoss MJ (2002) Shotgun proteomics: tools for the analysis of complex biological systems. Curr Opin Mol Ther 4:242–250
86. Druzhinina IS, Shelest E, Kubicek CP (2012) Novel traits of *Trichoderma* predicted through the analysis of its secretome. FEMS Microbiol Lett 337:1–9
87. Vodisch M, Scherlach K, Winkler R, Hertweck C, Braun HP, Roth M, Haas H, Werner ER, Brakhage AA, Kniemeyer O (2011) Analysis of the *Aspergillus fumigatus* proteome reveals metabolic changes and the activation of the pseurotin A biosynthesis gene cluster in response to hypoxia. J Proteome Res 10:2508–2524
88. Adav SS, Chao LT, Sze SK (2012) Quantitative secretomic analysis of *Trichoderma reesei* strains reveals enzymatic composition for lignocellulosic biomass degradation. Mol Cell Proteomics 11:1
89. Rodriguez A, Perestelo F, Carnicero A, Regalado V, Perez R, De la Fuente G, Falcon MA (1996) Degradation of natural lignins and lignocellulosic substrates by soil-inhabiting fungi imperfecti. FEMS Microbiol Ecol 21:213–9
90. Sutherland JB, Pometto AL, Crawford DL (1983) Lignocellulose degradation by *Fusarium* species. Can J Bot 61:1194–8
91. Edwards KJ, Gihring TM, Banfield JF (1999) Seasonal variations in microbial populations and environmental conditions in an extreme acid mine drainage environment. Appl Environ Microbiol 65:3627–3632
92. Reddy MS, Kumar S, Babita K, Reddy MS (2002) Biosolubilization of poorly soluble rock phosphates by *Aspergillus tubingensis* and *Aspergillus niger*. Biores Tech 84:187–9
93. Krishna P, Reddy MS, Patnaik SK (2005) *Aspergillus tubingensis* reduces the pH of the bauxite residue (red mud) amended soils. Water Air Soil Poll 167:201–9